Mol. Cells *28*, 175-181, September 30, 2009
DOI/10.1007/s10059-009-0120-1

Molecules and Cells

Proteomic Analysis of the Triglyceride-Rich Lipoprotein-Laden Foam Cells

Yanjun Lu, Jianli Guo, Yong Di, Yiqiang Zong, Shen Qu, and Jun Tian*

In hypertriglyceridaemic individuals, atherosclerogenesis is associated with the increased concentrations of very low density lipoprotein (VLDL) and VLDL-associated remnant particles. *In vitro* studies have suggested that VLDL induces foam cells formation. To reveal the changes of the proteins expression in the process of foam cells formation induced by VLDL, we performed a proteomic analysis of the foam cells based on the stimulation of differentiated THP-1 cells with VLDL. Using two-dimensional gel electrophoresis (2-DE) and matrix-assisted laser-desorption ionization time-of-flight mass spectrometry (MALDI-TOF MS) analysis, 14 differentially expressed proteins, containing 8 up-regulated proteins and 6 down-regulated proteins were identified. The proteins are involved in energy metabolism, oxidative stress, cell growth, differentiation and apoptosis, such as adipose differentiation-related protein (ADRP), enolase, S100A11, heat shock protein 27 and so on. In addition, the expression of some selected proteins was confirmed by Western blot and RT-PCR analysis. The results suggest that VLDL not only induces lipid accumulation, but also brings about foam cells diverse characteristics by altering the expression of various proteins.

INTRODUCTION

Hypertriglyceridemia has been as an independent risk factor for premature coronary artery disease (Hokanson and Austin, 1996). Atherosclerogenesis in hypertriglyceridaemic individuals is associated with the increased concentrations of VLDL and VLDL-associated remnant particles (Austin, 1999). A number of studies have shown that VLDL particles can enter the vascular wall and contribute directly to the accumulation of both extracellular and intracellular lipids (Frank and Fogelman, 1989; Nordestgaard et al., 1995). Furthermore, *in vitro* study has suggested that VLDL can induce foam cells formation (Evans et al., 1993; Rapp et al., 1994). However, compared with intensive research on the foam cells caused by modified low density lipoprotein (LDL), the characteristics of foam cells induced by VLDL still need to be illustrated.

VLDL is a large lipoprotein particle that is composed of triglycerides, free and esterified cholesterol, phospholipids, and apolipoproteins (Shelness and Sellers, 2001). Previous studies have indicated that the processing of internalized triglyceride-rich VLDL differs from the endocytotic route of LDL. VLDL causes lipid accumulation via a 2-step process. Initially, it interacts with cell surface lipoprotein lipase (LPL), which hydrolyzes core triglyceride to free fatty acids, which are then taken up by the cells and reesterified into triglyceride, finally the cholesteryl ester-rich remnants are readily taken up by receptor-mediated endocytosis (Argmann et al., 2001). In addition to causing lipid accumulation, increasing evidence suggests that VLDL has diverse roles in atherosclerosis (Byrne, 1999). Recent research has demonstrated that hydrolysis of VLDL by LPL can activate peroxisome proliferator-activated receptors (PPARs), preferential PPARα and PPARδ, which have been known to regulate the expression of the genes that are involved in lipid metabolism, glucose homeostasis and inflammation (Ricote et al., 2004). Apart from activating PPARs, VLDL can also activate the pivotal transcriptional regulator of nuclear factor-kappaB (NF-κB) (Dichtl et al., 1999). Even without prior oxidative modification, VLDL can potentiate inflammation molecule tumor necrosis factor expression (Stollenwerk et al., 2005) and increase IL-1β secretion in macrophages (Persson et al., 2006). Thus, revealing the characteristics of the VLDL-laden foam cells will help us to understand completely the atherosclerogenesis in hypertriglyceridaemic individuals.

The THP-1 human monocytic cell line is a well-characterized model system for studying the transformation of macrophages. When induced by phorbol 12-myristate 13-acetate (PMA), THP-1 monocytes can undergo differentiation into a macrophage-like phenotype which can then be converted into foam cells with the incubation of lipoproteins.

Proteomics offers a unique means for revealing the changes of the proteins expression profiles in the process of foam cell formation, providing the probable biomarkers in atherosclerosis. In this study, we carried out a proteomic analysis to characterize the foam cells derived from VLDL-laden THP-1 macrophages. Since it has been well known that foam cells are differentiated from macrophages by oxidized LDL (oxLDL), in the following experiments, oxLDL-laden THP-1 macrophages were performed as a positive control. Some proteins involving lipid accumulation, energy metabolism, oxidative stress, cell growth, differentiation and apoptosis were identified by MALDI-TOF MS. These changes in the proteins expression suggest that the complex biologic processes have occurred in macrophages

Department of Biochemistry and Molecular Biology, Tongji Medical College, Huazhong University of Science and Technology, Wuhan, People's Republic of China
*Correspondence: shjys@mails.tjmu.edu.cn

Received April 21, 2009; revised July 1, 2009; accepted July 22, 2009; published online September 7, 2009

Keywords: atherosclerogenesis, foam cell, proteomics, THP-1 cell, very low density lipoprotein

after treatment with VLDL.

MATERIALS AND METHODS

Reagents

PMA and thiourea were purchased from Sigma (USA). Immobiline DryStrips (IPG strips), carrier ampholytes (IPG buffers), iodoacetamide and CHAPS were purchased from GE Healthcare (USA). Trizol for RNA isolation was from Invitrogen (USA). Oil red O and Coomassie Brilliant Blue R-250 (CBB-R250) were obtained from Amersco (Sweden).

VLDL isolation, LDL isolation and oxidization

VLDL (d < 1.006 g/ml) and LDL (d = 1.006-1.063 g/ml) were isolated as previously described (Redgrave et al., 1975). Briefly, the human plasma was obtained from healthy volunteers and lipoproteins were prepared by discontinuous KBr gradient ultracentrifugation (60,000 × *g*, 7 h). The fraction including VLDL and the fraction including LDL were isolated and dialyzed against PBS including 1 mM EDTA, then sterilized by filtration through a 0.45 μm filter, and stored at 4°C. The isolated LDL was oxidized with CuSO4 (10 μM) for 18 h at 37°C, and dialyzed against PBS including 1 mM EDTA. The concentration of proteins was determined by the methods of Lowry (Pierce, USA).

Cell culture

The human monocytic cell THP-1 was obtained from the American Type Culture Collection (USA). The cells were cultured in a 5% CO_2 atmosphere in RPMI-1640 medium supplemented with 10% fetal bovine serum (FBS). The THP-1 cells were transformed into macrophage-like cells by induction of 0.2 μM PMA at 37°C for 48 h. After treatment with PMA, THP-1 macrophages were washed 3 times with PBS and incubated with fresh RPMI-1640 without serum for 24 h, and then stimulated with VLDL (50 μg/ml), oxLDL (50 μg/ml) or PBS in serum-free medium for 48 h.

Oil red O staining and lipid analysis

THP-1 cells were seeded on cover glasses and differentiated after induction by PMA for 2 d. The differentiated cells were then incubated with VLDL, oxLDL or PBS and serum-free media for 2 d and then fixed with 4% formaldehyde for 15 min. Cell lipids were stained with Oil red O (3 mg/ml in 60% isopropanol) for 10 min and then observed under a microscope. The images were captured on a Nikon Eclipse E800 microscope (Nikon, Japan) using NISElements software. Cellular cholesterol and triglyceride were determined by an enzymatic method as previously described (Carr et al., 1993).

Sample preparation and quantification

Cells after incubation with VLDL, oxLDL or PBS for 48 h were harvested by centrifugation at 4°C (1,000 × *g*, 5 min). The supernatants were discarded and the pellets were washed twice with PBS. Then the cells were suspended in lysis buffer containing 7 M urea, 2 M thiourea and 4% CHAPS for 30 min on ice and sonicated for 30 s with pulses 3 to 4 times until a clear solution was obtained. The resulting cell lysates were centrifuged at 20,000 × *g* for 60 min and the supernatants were collected. Protein concentration was determined using the PlusOne™ 2-D Quant kit (GE Healthcare, USA).

2-DE

Linear IPG 18 cm strips (pH 3-10) were rehydrated with the whole-cell protein samples for 12 h at 30 V using the IPGphor II apparatus (GE Healthcare, USA). Isoelectric focusing was performed for a total of 48 kV/h, according to the manufacturer's instructions. Prior to SDS-PAGE, strips were equilibrated for 15 min in 50 mM Tris-HCl (pH 8.8), 6 M urea, 30% glycerol, 2% SDS containing 65 mM DTT, and then for a further 15 min in the same buffer containing 240 mM iodoacetamide. Equilibrated strips were transferred onto 12.5% SDS-PAGE. Strips were overlaid with 0.5% low-melting point agarose in running buffer containing bromophenol blue. Gels were run in aHoefer DALT™ tank using the Ettan DALT*six* electrophoresis system (GE Healthcare, USA) at 2 W/gel for approximately 1 h and then at 17 W/gel for about 5 h in running buffer containing 25 mM Tris, 192 mM glycine and 0.1% SDS. Following electrophoresis, the gels were stained with CBB-R 250 (50% methanol, 10% glacial acetic acid and 0.1% CBB-R 250) for 12 h and then destained overnight in 10% methanol and 10% glacial acetic acid. Gels were washed twice with water and imaged using Image Scanner and Lab scan V.5 software (GE Healthcare, USA), and finally the gels were analyzed with Image Master Platinum software (GE Healthcare, USA). Spots of interest were excised manually, cut into pieces and stored at -20°C for protein identification.

Protein identification by MALDI-TOF MS

The spot pieces were destained twice with 60 μl, 200 mM NH_4HCO_3/ACN (50:50 v/v) and the supernatants were discarded. Then, the gel pieces were air dried and digested overnight at room temperature using 20 ng/ml trypsin. The peptides extracted from the gel pieces using 50% ACN and 0.1% TFA were dried overnight and then dissolved in 3 ml of 50% ACN, 0.1% TFA mixed with 3 ml of a CHCA matrix, and 1 ml of which was spotted onto the MALDI-TOF target plate. The peptide mass fingerprinting (PMF) was acquired using a Bruker-Daltonics AutoFlex TOF-TOF LIFT MS (Bruker, German). The database search was carried out by the MASCOT search engine, using a peptide tolerance of 50 ppm.

Western blot analysis

Following cell protein quantitation, whole protein extracts (60-80 μg) from treated cells were subjected to 12.5% SDS-PAGE. Proteins were then transferred to a nitrocellulose membrane, for ADRP, enolase, S100A11, phosphoglycerate mutase 1 (PGAM1) immunodetection, membranes were blocked for 1 h at room temperature in TBST (50 mM Tris-HCl, pH 7.6, 150 mM NaCl, 0.1% Tween 20) and 5% nonfat dried milk, and then incubated with mouse monoclonal anti-human ADRP (Boster, China) antibody (1:200 in blocking buffer, overnight at 4°C), mouse monoclonal anti-S100A11 (ProteinTech, USA) antibody (1:800 in blocking buffer, overnight at 4°C), rabbit polyclonal anti-human enolase (ProteinTech, USA) antibody (1:1000 in blocking buffer, overnight at 4°C), rabbit monoclonal PGAM1 (Abcam, UK) (1:1000 in blocking buffer, overnight at 4°C). The membranes were incubated with the appropriate secondary antibody for 1 h at room temperature and the proteins were visualized with an ECL detection system (Pierce, USA). The densities of immunoreactive bands were measured by the Image Quant TL software (GE Healthcare, USA).

RT-PCR analysis

After treatment with VLDL or PBS, total RNA of the cells was isolated using Trizol reagent according to the manufacturer's instructions. Total RNA (8 μg) from each sample was subjected to reverse transcription with oligdT, dNTPs and M-MLV reverse transcriptase in a 20 μl total reaction volume. PCR was performed using specific primers for the proteins of interest and the

Table 1. Conditions for PCR amplification of the genes studied

Target gene	PCR primers	Annealing temp (°C)	Number of cycles	Product size (bp)
ADRP	Forward: 5′-AGGGGCTAGACAGGATTGAGGA-3′			
	Reverse: 5′-TTTTCTACGCCACTGCTCACG-3′	53	28	280
enolase 1	Forward: 5′- CGCATTGGAGCAGAGGTTTAC-3′			
	Reverse: 5′-GCAGTTGCAGGACTTCTCGTT-3′	52	27	471
PGAM1	Forward: 5′-GAGCCCGACCATCCTTTCTACA-3′			
	Reverse: 5′-AATACCAGTCGGCAGGTTCAGC-3′	54	30	264
S100A11	Forward: 5′-GTCCCTGATTGCTGTCTTCC-3′			
	Reverse: 5′-ACCAGGGTCCTTCTGGTTCT-3′	52	25	130

genes amplification primer sequences were listed in Table 1. The PCR products identified by 2% agarose gel electrophoresis were analyzed using Image Quant TL software. All samples were analyzed in triplicate.

RESULTS

VLDL induce massive triglycerides accumulation in THP-1 macrophages

In order to observe the effect of VLDL or oxLDL on the content of cellular lipids, the cell lipids were stained with Oil red O. As shown in Fig. 1A, the content of cellular lipids of the cells treated with VLDL or oxLDL was significantly higher than that treated with PBS. Furthermore, the cellular lipids were quantified. VLDL caused lipid accumulation, major as triglycerides in the THP-1 macrophages. The concentration of triglyceride in VLDL-treated cells was significantly higher than that in PBS-treated cells (5.6 fold) (Fig. 1B). While oxLDL caused lipid accumulation, major as cholesterol (4.4 fold compared with PBS-treated cells) (Fig. 1B). The total cholesterol in VLDL-treated cells and total triglyceride in oxLDL-treated cells were increased 1.4 fold and 1.7 fold compared with PBS-treated cells, respectively (Fig. 1B).

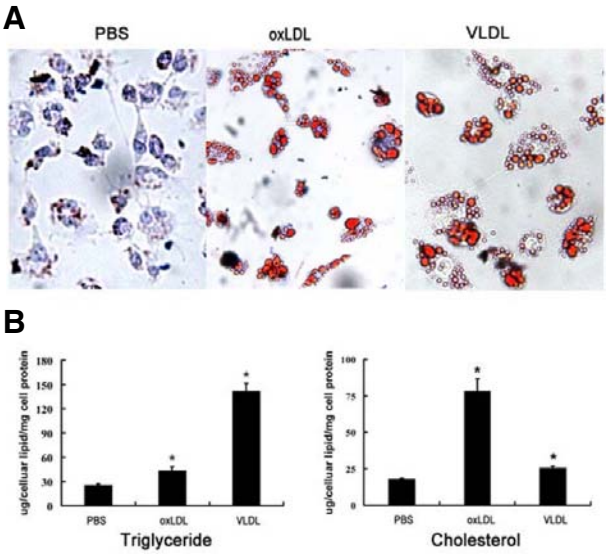

Fig. 1. (A) Oil red O staining of the THP-1 macrophages after the treatment with PBS, oxLDL (50 μg/ml) or VLDL (50 μg/ml) for 2 d. All images were originally magnified 60·fold. (B) Quantification of the cellular lipid. The left panel showed the concentration of triglyceride in the cells treated with PBS, oxLDL or VLDL. The right panel showed the concentration of cholesterol in the cells treated with PBS, oxLDL or VLDL. The significant difference of values from the treatment with PBS was determined by Student's *t*-test (*$P < 0.05$), and the data represent the mean ± SD from three independent experiments performed in triplicate.

Proteomics analysis of foam cell treated with VLDL or oxLDL

The total proteins of the THP-1 macrophages treated with VLDL or oxLDL were extracted and separated by 2-DE. To obtain statistically significant results, each protein sample run in triplicate. Representative 2-DE gel images for the cells treated with PBS, oxLDL or VLDL were depicted in Fig. 2A. Following image analysis, over 1,000 protein spots were clearly separated on each gel, ranging from 6-150 kDa between pH 3-10. Comparative analysis of the gels between VLDL-treated cells and PBS-treated cells showed that 114 spots were up-regulated and 101 spots were down-regulated. While comparative analysis of the gels between oxLDL-treated cells and PBS-treated cells showed that 128 spots were up-regulated and 115 spots were down-regulated. Then we compared the differentially expressed proteins between VLDL-treated cells and PBS-treated cells with the differentially expressed proteins between oxLDL-treated cells and PBS-treated cells, 54 spots both in oxLDL-treated and in VLDL-treated cells were up-regulated compared with that in PBS-treated cells, 37 spots both in oxLDL-treated and in VLDL-treated cells were down-regulated compared with that in PBS-treated cells. The others or did not match, and had their own unique changes, either matched, but the changes in the opposite. After analysis, 8 significantly increased proteins and 6 significantly decreased proteins (fold change >1.4) in VLDL-treated THP-1 macrophages were identified by MALDI-TOF MS. The results were listed in Table 2. The positions of the identified protein spots in corresponding gels were shown in Fig. 2A. Direct comparison of the relative expression level of protein spots among the cells treated with PBS, oxLDL or VLDL was illustrated in Fig. 2B. The identified proteins were grouped into the following categories according to their biological functions: lipid accumulation, energy metabolism, oxidative stress, cell growth, differentiation and apoptosis.

Validation of the selected proteins by Western blot and RT-PCR analysis

To validate the proteomic data, we also performed Western blot and RT-PCR analysis of four selected proteins including ADRP, PGAM1, enolase and S100A11. As shown in Fig. 3, the expression of ADRP protein in oxLDL-treated cells or in VLDL-

Table 2. Spots identified by MALDI-TOF MS

No	NCBInr	Name	Sequence coverage	Theoritic MW (Da)	Theoritic PI	Observed MW (kDa)	Observed PI	Score	Match
1	gi|34577059	adipose differentiation-related protein	40%	48274	6.34	52	7.5313	164	13/22
2	gi|4503571	enolase 1	49%	47481	7.01	51	8.03003	223	17/28
3	gi|2781202	Chain A, Three-Dimensional Structure Of Human Electron Transfer Flavoprotein To 2.1 A Resolution	49%	33418	6.95	35	8.14046	167	12/22
4	gi|4505753	phosphoglycerate mutase 1	50%	28900	6.67	32	7.31043	124	8/14
5	gi|5032057	S100 calcium binding protein A11	89%	11847	6.56	13	6.68346	93	10/50
6	gi|1633054	Chain A, Cyclophilin A Complexed With Dipeptide Gly-Pro	52%	18098	7.82	18	9.07023	95	7/9
7	gi|18490229	DMGDH protein	20%	69463	6.16	12	8.79593	76	9/26
8	gi|4504517	heat shock 27kDa protein 1	52%	22826	5.98	30	6.72265	157	10/21
9	gi|119569783	peroxiredoxin 3, isoform CRA_c	43%	11158	6.06	25	6.94351	70	4/9
10	gi|119577230	heterogeneous nuclear ribonucleoprotein L, isoform CRA_a	19%	60693	6.81	62	7.83766	98	9/15
11	gi|46593007	ubiquinol-cytochrome c reductase core protein I	28%	53297	5.94	61	5.84631	110	10/20
12	gi|70995211	peroxisomal enoyl-coenzyme A hydratase-like protein	28%	36136	8.16	36	7.37099	104	7/11
13	gi|119590499	fumarate hydratase, isoform CRA_d	35%	46555	6.9	50	8.52875	141	10/12
14	gi|119610226	fructosamine 3 kinase, isoform CRA_b	21%	50553	9.48	40	8.11552	49	10/38

treated cells was significantly increased 1.3 fold or 2.7 fold, respectively, compared with that in PBS-treated cells (Fig. 3A), S100A11 protein level increased 1.8 fold in VLDL-treated cells, while decreased 1.2 fold in oxLDL-treated cells (Fig. 3D). On the contrary, both PGAM1 and enolase were down-regulated in oxLDL-treated cells or in VLDL-treated cells. PGAM1 decreased approximately 1.7 fold or 1.8 fold, respectively, and enolase decreased approximately 1.5 fold or 1.7 fold, respectively (Figs. 3B and 3C). The changes in the mRNA level of the four selected genes in VLDL-treated cells were shown in Fig. 4, ADRP mRNA significantly increased 3.5 fold in VLDL-treated cells compared with PBS-treated control cells (Fig. 4A) and S100A11 mRNA expression increased about 1.5 fold (Fig. 4D). On the contrary, enolase mRNA expression decreased 2.5 fold and PGAM1 decreased 3.3 fold, respectively (Figs. 4B and 4C).

DISCUSSION

Hypertriglyceridemia is a strong risk factor for the development of coronary heart disease. Recent experiments in mouse models of atherosclerosis have found an increased susceptibility to atherosclerosis with high VLDL levels (Vanderlaan et al., 2009). However, the role of VLDL-laden foam cells in atherosclerosis is not clear. Thus, we carried out a proteomic analysis to reveal the characteristics of the triglyceride-rich foam cells in atherosclerosis.

Lipid droplets are a defining feature of foam cells, which are ubiquitous organelles involved in the storage and turnover of neutral lipids such as triglycerides (Persson et al., 2007). In this study, THP-1 macrophages treated with VLDL for 48 h accumulated massive lipid droplets, major as triglycerides. However, almost no lipid droplets were observed in the cells treated with PBS. Furthermore, ADRP identified in our study which is associated with lipid droplet was over-expressed in VLDL-laden foam cells. ADRP plays a central role in the formation of lipid droplets (Brasaemle et al.,1997; Imamura et al., 2002), which promotes the storage of triglycerides in the lipid droplets by increasing the uptake of saturated, monounsaturated or polyunsaturated long-chain fatty acids (Gao and Serrero, 1999) and by inhibiting its β-oxidation (Larigauderie et al., 2006). It has been reported that VLDL can up-regulate ADRP mRNA expression in the macrophages through PPARδ, which is activated by the triglycerides, the components of VLDL (Chawla et al., 2003). ADRP mRNA in VLDL-treated cells increased 3.5 fold compared with that in PBS-treated cells. The result supports that VLDL regulates ADRP expression at transcriptional level.

PGAM1 and enolase identified which are associated with glucose metabolism were down-regulated in the process of foam cells formation. PGAM1 catalyzes the interconversion of 3-phosphoglycerate to 2-phosphoglycerate and enolase catalyzes the generation of phosphoenolpyruvate from 2-phosphoglycerate. It has been reported that human triglyceride-rich lipoproteins can impair glucose metabolism in L6 skeletal muscle cells (Pedrini et al., 2005). The cellular glucose measured in VLDL-treated (50 μg/ml) macrophages was increased (3.2 fold compared with PBS-treated cells, the data not shown). The elevation of glucose and down-regulation of the two glycolytic enzymes probably suggested that the celluar glucose utilization via glycolysis was reduced. It has been described that glucose utilization is inhibited by 65 ± 7% in human aortic smooth muscle cells (HASMC) treated with oxLDL compared with the cells incubated in lipid-free media, associated with the down-regulated glycolytic enzyme glyceraldehyde-3-phosphate dehydrogenase (GAPDH) (Sukhanov et al., 2006). It has been

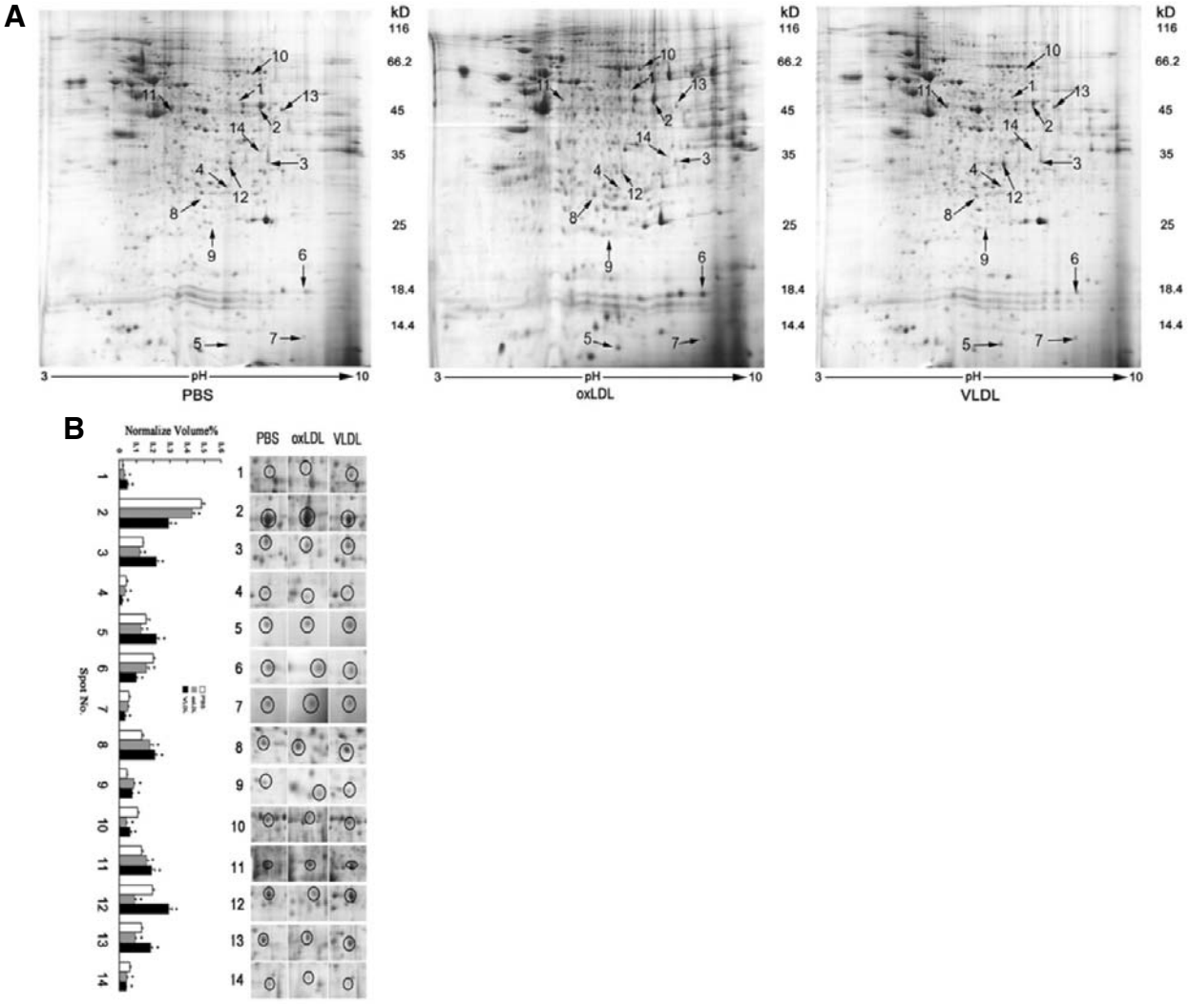

Fig. 2. Differential protein profiling of the cells treated with oxLDL or VLDL compared with the cells treated with PBS. (A) Two-dimensional gel protein expression maps of the cells treated with PBS, oxLDL or VLDL. All spots identified by MALDI-TOF MS after CBB-R 250 staining were present in the corresponding gels, the arrows showed the positions of all 14 protein spots that had been shown to be significantly altered caused by VLDL or oxLDL. The identified spots were listed in Table 2. (B) Direct comparison of differentially expressed proteins derived from the cells induced by oxLDL or VLDL with that induced by PBS in the representative two-dimensional gels (right panel). The left panel showed the corresponding bar charts of relative expression level of spots derived from the cells treated with PBS, oxLDL or VLDL. A statistically significant difference of values from the treatment with PBS was analyzed by using Student's *t*-test (*$p < 0.05$). The data represent the mean ± SD from three independent experiments performed in triplicate.

reported that the two glycolytic enzymes are also down-regulated in the white adipose tissues of mice with high fat feeding (Schmid et al., 2004). The down-regulation of these glycolytic enzymes may be a result of a competition for an oxidative fuel source between fatty acids and glucose in the VLDL-laden macrophages.

Ubiquinol-cytochrome C reductase core protein 1 (an oxidative phosphorylation III subunit) and chain a, three-dimensional structure of human electron transfer flavor protein to 2.1A resolution as part of the mitochondrial respiratory chain identified were also up-regulated. The ubiquinol-cytochrome C reductase complex catalyzes electron transfer from ubiquinol to cytochrome C. Recent research has pointed out that cellular reactive oxygen species (ROS) levels are strongly elevated in the J774.2 macrophages treated with triglycerides. The triglyceride-mediated ROS are derived from mitochondrial complex 1 of the electron-transfer chain (Aronis et al., 2005). It is known that the mitochondrial respiratory chain is the major source of superoxide anion (Han et al., 2001). Mitochondrial dysfunction and oxidative stress have been viewed as common risk factors for atherosclerosis (Alexander, 1998). In our study, these over-expressed proteins were probably associated with the products of superoxide anion derived from mitochondria. It has been reported that fatty acid, the hydrolytic product of triglyceride, induces antioxidant effect by activating cellular glutathione peroxidase and subsequently enhances ROS degradation (Duval et al., 2002). The protein peroxidase III localized in mitochondria identified was up-regulated in our study and the change maybe serves as a feedback defense to the increased oxidative stress status in the treated cells. Thus, the results support the hypothesis that triglyceride or the main form of VLDL is the main

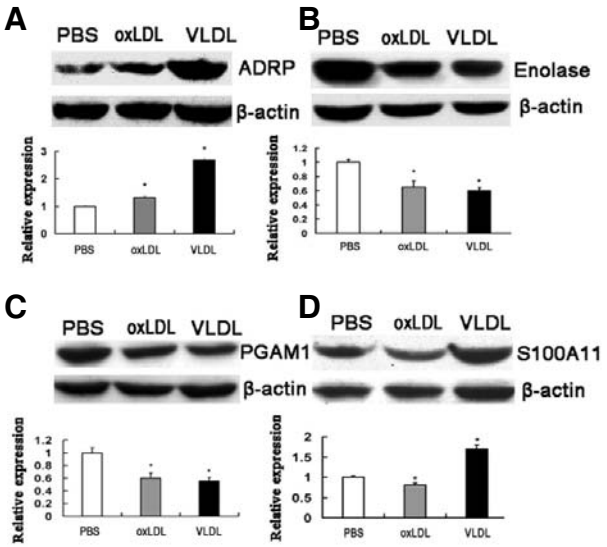

Fig. 3. Western blotting analysis of four selected proteins in the THP-1 macrophages incubated with PBS, oxLDL (50 μg/ml) or VLDL (50 μg/ml) for 2 d. The bands were analyzed using Image Quant TL software. The amount of selected proteins was normalized with internal standard β-actin. The significant difference of values from the treatment with PBS was determined by Student's *t*-test (*P < 0.05), and the data represent the mean ± SD from three independent experiments performed in triplicate.

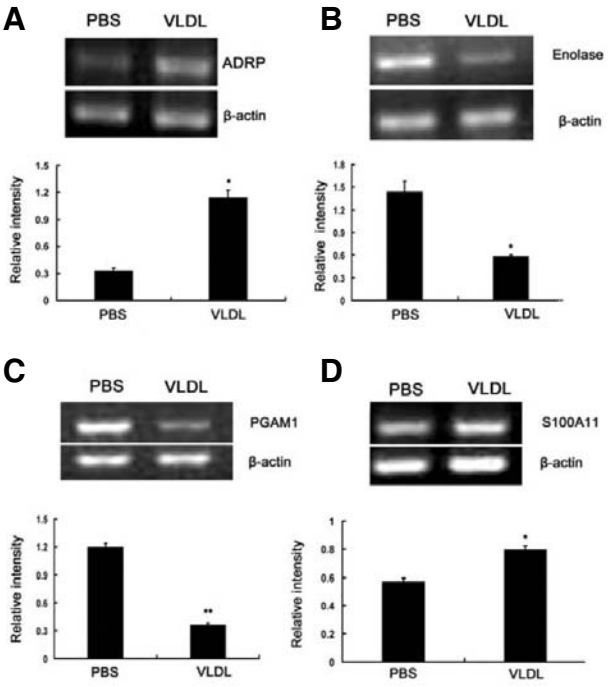

Fig. 4. Quantitative RT-PCR analysis of four selected genes in the THP-1 macrophages incubated with PBS or with VLDL (50 μg/ml) for 2 d. Agarose gel bands were analyzed using Image Quant TL software. The significant difference of values from the treatment with PBS was determined by Student's *t*-test (*P < 0.05, **P < 0.01), and the data represent the mean ± SD from three independent experiments performed in triplicate.

cause of the oxidative stress in atherosclerotic plaque derived from the high fat feeding.

The down-regulated extracellular heat shock protein 27 (HSP27) has been reported as a biomarker in atherosclerosis (Martin-Ventura et al., 2004), while it was increased in the process of form cells formation in the study. Small intracellular heat shock proteins are involved in different processes, such as the response to stress and modulation of the actin cytoskeleton or apoptosis. Up-regulation of some of these proteins ensures the maintenance of cell homeostasis and survival. It has been reported that when plasmin-treated vascular smooth muscle cells (VSMCS) were treated with HSP27 siRNA, the rate of VSMCS apoptosis is increased (Martin-Ventura et al., 2006), which suggests that intracellular HSP27 has an anti-apoptotic effect. However, the precise role of HSP27 in the process of foam cells formation remains to be elucidated.

S100A11 identified was significantly up-regulated in the macrophages treated with VLDL, which has not been reported in previous research on foam cells. S100A11 belongs to S100 family of Ca^{2+} binding proteins which is abundant in the placenta, highly expressed in human heart, lung, kidney, uterus, bladder, prostate and skeletal muscle, and poorly expressed in other tissues (Inada et al., 1999). A few reports have shown that S100A11 is up-regulated in tumor tissues and plays a role in cell growth, differentiation and apoptosis (Kanamori et al., 2004; Memon et al., 2005). It has been shown that the macrophage foam cells proliferate in cholesterol-fed New Zealand rabbits (Rosenfeld and Ross, 1990). Another report has indicated that murine macrophages show stimulated growth when challenged with modified LDL, such as oxLDL and acetylated LDL, in vitro (Gordon et al., 1990). Maybe the elevation of S100A11 is related to the proliferation of macrophages induced by VLDL.

In this study, a comparative proteomic technology was used to reveal the changes of the proteome in the foam cells from VLDL-laden macrophages, some interesting proteins related to the lipid accumulation, energy metabolism, oxidative stress, cell growth, differentiation and apoptosis were identified. The changes in these proteins expression have partly revealed the complex biologic characteristic of the macrophages after treatment with VLDL. Compared with previous research on the foam cells derived from the cholesterol-rich lipoprotein-laden macrophages, these changes are probably associated with the inherent characteristics of VLDL. To our knowledge, this is the first time to characterize triglyceride-rich foam cells using a proteomic strategy.

ACKNOWLEDGMENT

This work was supported by the National Natural Science Foundation of China (No.30470872, 30300134).

REFERENCES

Alexander, R.W. (1998). Atheroscleros is as a disease of redox-sensitive genes. Trans. Am. Clin Climatol. Assoc. *109*, 129-146.

Argmann, C.A., Van Den Diepstraten, C.H., Sawyez, C.G., Edwards, J.Y., Hegele, R.A., Wolfe, B.M., and Huff, M.W. (2001). Transforming growth factor-β1 inhibits macrophage cholesteryl ester accumulation induced by native and oxidized VLDL remnants. Arterioscler. Thromb. Vasc. Biol. *21*, 2011-2018.

Aronis, A., Madar, Z., and Tirosh, Q. (2005). Mechanism underlying oxidative stress-mediated lipotoxicity: exposure of J774.2 macrophages to triacylglycerols facilitates mitochondrial reactive oxygen species production and cellular necrosis. Free Radic. Biol. Med. *38*, 1221-1230.

Austin, M.A. (1999). Epidemiology of hypertriglyceridemia and cardiovascular disease. Am. J. Cardiol. *83*, 13F-16F.

Brasaemle, D.L., Barber, T., Wolins, N., Serrero, G., Blanchette, E.J., and Londos, C. (1997). Adipose differentiation-related protein is an ubiquitouslyexpressed lipid storage droplet associated protein. J. Lipid Res. *38*, 2249-2263.

Byrne, C.D. (1999). Triglyceride-rich lipoproteins: are links with atherosclerosis mediated by a procoagulant and proinflammatory phenotype? Atherosclerosis *145*, 1-15.

Carr, T.P., Andresen. C.J., and Rudel, L.L. (1993). Enzymatic determination of triglyceride, free cholesterol, and total cholesterol in tissue lipid extracts. Clin. Biochem. *26*, 39-42.

Chawla, A., Lee, C.H., Barak, Y., He, W., Rosenfeld, J., Liao, D., Han, J., Kang, H., and Evans, R.M. (2003). PPARδ is a very low-density lipoprotein sensor in macrophages. Proc. Natl. Acad. Sci. USA *100*, 1268-1273.

Dichtl, W., Nilsson, L., Goncalves, I., Ares, M.P., Banfi, C., Calara, F., Hamsten, A., Eriksson, P., and Nilsson, J. (1999). Very low-density lipoprotein activates nuclear factor-kappaB in endothelial cells. Circ. Res. *84*, 1085-1094.

Duval, C., Augé, N., Frisach, M.F., Casteilla, L., Salvayre, R., and Nègre-Salvayre, A. (2002). Mitochondrial oxidative stress is modulated by oleic acid via an epidermal growth factor receptor-dependent activation of glutathione peroxidase. Biochem. J. *367*, 889-894.

Evans, A.J., Sawyez, C.G., Wolfe, B.M., Connelly, P.W., Maguire, G.F., and Huff, M.W. (1993). Evidence that cholesteryl ester and triglyceride accumulation in J774.2 macrophages induced by very low density subfractions occurs by different mechanisms. J. Lipid Res. *34*, 703-717.

Frank, J.S., and Fogelman, A.M. (1989). Ultrastructure of the intima in WHHL and cholesterol-fed rabbit aortas prepared by ultrarapid freezing and freeze-etching. J. Lipid Res. *30*, 967-978.

Gao, J., and Serrero, G. (1999). Adipose differentiation related protein (ADRP) expressed in transfected COS-7 cells selectively stimulates long chain fatty acid uptake. J. Biol. Chem. *274*, 16825-16830.

Gordon, D., Reidy, M.A., Benditt, E.P., and Schwartz, S.M. (1990). Cell proliferation in human coronary arteries. Proc. Natl. Acad. Sci. USA *87*, 4600-4604.

Han, D., Williams, E., and Cadenas, E. (2001). Mitochondrial respiratory chain-dependent generation of superoxide anion and its release into the intermembrane space. Biochem. J. 2001, *353*, 411-416.

Hokanson, J.E., and Austin, M.A. (1996). Plasma triglyceride level is a risk factor for cardiovascular disease independent of high density lipoprotein cholesterol levels: a meta-analysis of population-based prospective studies. J. Cardiovasc. Risk *3*, 213-219.

Imamura, M., Inoguchi, T., Ikuyama, S., Taniguchi, S., Kobayashi, K., Nakashima, N., and Nawata, H. (2002). ADRP stimulates lipid accumulation and lipid droplet formation in murine fibroblasts. Am. J. Physiol. Endocrinol. Metab. *283*, 775-783.

Inada, H., Naka, M., Tanaka, T., Davey, G.E., and Heizmann, C.W. (1999). Human S100A11 exhibits differential steady-state RNA levels in various tissues and a distinct subcellular localization. Biochem. Biophys. Res. Commun. *263*, 135-138.

Kanamori, T., Takakura, K., Mandai, M., Kariya, M., Fukuhara, K., Sakaguchi, M., Huh, N.H., Saito, K., Sakurai, T., Fujita, J., et al. (2004). Increased expression of calcium-binding protein S100 in human uterine smooth muscle tumours. Mol. Hum. Reprod. *10*, 735-742.

Larigauderie, G., Cuaz-Pérolin, C., Younes, A.B., Furman, C., Lasselin, C., Copin, C., Jaye, M., Fruchart, J.C., and Rouis, M. (2006). Adipophilin increases triglyceride storage in human macrophages by stimulation of biosynthesis and inhibition of b-oxidation. FEBS J. *273*, 3498-3351.

Martin-Ventura, J.L., Duran, M.C., Blanco-Colio, L.M., Meilhac, O., Leclercq, A., Michel, J.B., Jensen, O.N., Hernandez-Merida, S., Tuñón, J., Vivanco, F., et al. (2004). Identification by a differential proteomic approach of heat shock protein 27 as a potential marker of atherosclerosis. Circulation *110*, 2216-2219.

Martin-Ventura, J.L., Nicolas, V., Houard, X., Blanco-Colio, L.M., Leclercq, A., Egido, J., Vranckx, R., Michel, J.B., and Meilhac, O. (2006). Biological significance of decreased HSP27 in human atherosclerosis. Arterioscler. Thromb. Vasc. Biol. *26*, 1337-1343.

Memon, A.A., Sorensen, B.S., Meldgaard, P., Fokdal, L., Thykjaer, T., and Nexo, E. (2005). Down-regulation of S100C is associated with bladder cancer progression and poor survival. Clin. Cancer Res. *11*, 606-611.

Nordestgaard, B.G., Wootton, R., and Lewis, B. (1995). Selective retention of VLDL, IDL, and LDL in the arterial intima of genetically hyperlipidemic rabbits *in vivo*: Molecular size as a determinant of fractional loss from the intima-inner media. Arterioscler. Thromb. Vasc. Biol. *15*, 534-542.

Pedrini, M.T., Kranebitter, M., Niederwanger, A., Kaser, S., Engl. J., Debbage, P., Huber, L.A., and Patsch, J.R. (2005). Human triglyceride-rich lipoproteins impair glucose metabolism and insulin signalling in L6 skeletal muscle cells independently of non-esterified fatty acid levels. Diabetologia *48*, 756-766.

Persson, J., Nilsson, J., and Lindholm, M.W. (2006). Cytokine response to lipoprotein lipid loading in human monocyte-derived macrophages. Lipids Health Dis. *5*, 17-24.

Persson, J., Degerman, E., Nilsson, J., and Lindholm, M.W. (2007). Perilipin and adipophilin expression in lipid loaded macrophages. Biochem. Biophys. Res. Commun. *363*, 1020-1026.

Rapp, J.H., Lespine, A., Hamilton, R.L., Colyvas, N., Chaumeton, A.H., Tweedie-Hardman. J., and Kane, J.P. (1994). Triglyceride-rich lipoproteins isolated by selected affinity anti-apolipoprotein B immunosorption from human atherosclerotic plaque. Arterioscler Thromb Vasc. Biol. *14*, 1767-1774.

Redgrave, T.G., Roberts, D., and West, C.E. (1975). Separation of plasma lipoproteins by density-gradient ultracentrifugation. Anal. Biochem. *65*, 42-49.

Ricote, M., Valledor, A.F., and Glass, C.K. (2004). Decoding transcriptional programs regulated by PPARs and LXRs in the macrophage: effects on lipid homeostasis, Inflammation, and atherosclerosis. Arterioscler. Thromb. Vasc. Biol. *24*, 230-239.

Rosenfeld, M.E., and Ross, R. (1990). Macrophage and smooth muscle cell proliferation in atherosclerotic lesions of WHHL and comparably hypercholesterolemic fat-fed rabbits. Arteriosclerosis *10*, 680-687.

Schmid, G.M., Converset, V., Walter, N., Sennitt, M.V., Leung, K.Y., Byers, H., Ward, M., Hochstrasser, D.F., Cawthorne, M.A., and Sanchez, J.C. (2004). Effect of high-fat diet on the expression of proteins in muscle, adipose tissues, and liver of C57BL/6 mice. Proteomics *4*, 2270-2282.

Shelness, G.S., and Sellers, J.A. (2001). Very-low-density lipoprotein assembly and secretion. Curr. Opin. Lipidol. *12*, 151-157.

Stollenwerk, M.M., Schiopu, A., Fredrikson, G.N., Dichtl, W., Nilsson, J., and Ares, M.P. (2005). Very low density lipoprotein potentiates tumor necrosis factor-alpha expression in macrophages. Atherosclerosis. *179*, 247-254

Sukhanov, S., Higashi, Y., Shai, S.Y., Itabe, H., Ono, K., Parthasarathy, S., and Delafontaine, P. (2006). Novel effect of oxidized low-density lipoprotein: cellular ATP depletion via down-regulation of glyceraldehyde-3-phosphate dehydrogenase. Circ. Res. *99*, 191-200.

Vanderlaan, P.A., Reardon, C.A., Thisted, R.A., and Getz, G.S. (2009). VLDL best predicts aortic root atherosclerosis in low density lipoprotein receptor deficient mice. J. Lipid Res. *50*, 376-385.